Hindawi Publishing Corporation
Journal of Chemistry
Volume 2014, Article ID 739273, 12 pages
http://dx.doi.org/10.1155/2014/739273

Research Article

Utilization to Remove Pb (II) Ions from Aqueous Environments Using Waste Fish Bones by Ion Exchange

Bayram Kizilkaya[1] and A. Adem Tekınay[2]

[1] *Faculty of Marine Sciences and Technology, Canakkale Onsekiz Mart University, 17100 Canakkale, Turkey*
[2] *Faculty of Fisheries, Izmir Katip Celebi University, 35620 Cigli/Izmir, Turkey*

Correspondence should be addressed to Bayram Kizilkaya; bayram342001@yahoo.com

Received 2 May 2013; Revised 3 March 2014; Accepted 17 March 2014; Published 29 April 2014

Academic Editor: Huu Hao Ngo

Removal of lead (II) from aqueous solutions was studied by using pretreated fish bones as natural, cost-effective, waste sorbents. The effect of pH, contact time, temperature, and metal concentration on the adsorption capacities of the adsorbent was investigated. The maximum adsorption capacity for Pb (II) was found to be 323 mg/g at optimum conditions. The experiments showed that when pH increased, an increase in the adsorbed amount of metal of the fish bones was observed. The kinetic results of adsorption obeyed a pseudo second-order model. Freundlich and Langmuir isotherm models were applied to experimental equilibrium data of Pb (II) adsorption and the value of R_L for Pb (II) was found to be 0.906. The thermodynamic parameters related to the adsorption process such as E_a, ΔG°, ΔH°, and ΔS° were calculated and E_a, ΔH°, and ΔS° were found to be 7.06, 46.01 kJ mol^{-1}, and 0.141 kJ mol^{-1}K^{-1} for Pb (III), respectively. ΔH° values (46.01 kJmol^{-1}) showed that the adsorption mechanism was endothermic. Weber-Morris and Urano-Tachikawa diffusion models were also applied to the experimental equilibrium data. The fish bones were effectively used as sorbent for the removal of Pb (II) ions from aqueous solutions.

1. Introduction

The contamination with toxic metals is the most important problem facing all over the world. Lead is one of the most toxic metals for living species and people [1]. Many important industrial applications, such as storage battery, manufacturing, printing pigments, fuels, photographic materials, explosive manufacturing, metal plating, mining, painting, car manufacturing, smelters, and metal refineries [2, 3], are major sources of Pb (II) contamination [4]. Lead concentrations come near to 200–500 mg/L in many industrial wastewaters and it should be reduced to a range of 0.1–0.05 mg/L [5, 6]. Different removal methods such as chemical precipitation, ion exchange, membrane filtration, solvent extraction, phytoextraction, ultrafiltration, reverse osmosis, and adsorption have been used to remove heavy metals from water and wastewaters [7–10]. Many of these processes have some disadvantages such as deficient removal, high energy requirement, and new toxic sludge/waste products that need further treatment before disposal [6]. The adsorption procedure is a simple and low-cost method for metal removal [6]. Generally, cost-effective alternative sorbents for heavy metal removal from water resources can be obtained from materials which exist abundantly in nature or arise as byproducts and waste materials from various industries [8, 11]. Recently, researchers have reported that materials with biological and natural origins, such as agricultural, banana peel, peel waste, and animal waste, are effective and usable in the removal of metals [9, 12–16]. Some sorbents such as seaweed (*Gymnogongrus Torulosus*) [17], leaf powder (*Ficus religiosa*) [18], and bacteria (*Tannery Effluents Contaminated Soil*) [19] were used for metal removal. Bones are composed of 30% organic compounds and 70% inorganics by weight [20]. The inorganic phase consists mainly of hydroxyapatite $Ca_{10}(PO_4)_6(OH)_2$ (HAP) [11, 13]. HAP is an effective inorganic adsorption material because it has a high removal capacity for heavy metals by an ion exchange reaction with calcium ions on the bone surface. Animal bones, a source of biogenic apatite for

heavy metal removal, have been used as a sorbent source due to their low cost, natural abundance, and efficiency [11, 12, 21, 22].

In this study, the removal of Pb (II) ions from aqueous environments was investigated using pretreated fish bones. The bogue (*Boops boops*, Linnaeus 1758) bones were selected as a model fish bone for adsorption. The removal efficiency of the adsorbent was investigated as a function of pH, contact time, initial metal concentration, and temperature. Langmuir and Freundlich models were used to find the adsorption isotherms with the best fit to the experimental data. Weber-Morris and Urano-Tachikawa diffusion models were also applied to experimental equilibrium data. Thermodynamic parameters such as E_a, ΔG°, ΔH°, and ΔS° were calculated to determine the feasibility of the adsorption mechanism. *Desorption* studies were also carried out to demonstrate reusability of the bone sorbent.

2. Materials and Methods

2.1. Preparation and Pretreatment of Bone Sorbents. The fish (*Boops boops*) were obtained from local fish-shops in Canakkale (TURKEY). Firstly, fish bones were separated from meat and washed with hot distilled water several times. The cleaning procedures are applied at solid to liquid ratio 1 : 50 for two hours and cleaned with 0.1 M NaOH solution at 60°C and stirring rate 150 rpm, denoted as B [20]. The fish bones were dried in an oven at 50°C and then milled to particle sizes between 50 and 200 μm with a mortar.

2.2. Apparatus and Chemicals. FT-IR (Perkin Elmer FT-IR-Spectrum One, using ATR technique, 4000–550 cm^{-1}), SEM-EDX (Phillips XL-30S FEG, analyzed IYTE-Material Research Central/IZMIR), Carbon-Sulfur analyzer (LECO SC-144DR), ICP-AES (Varian Liberty II Series, Sequential Series-Axial, Australia), and Micromeritics-Gemini V for BET surface area were used for the characterization of bone sorbents. ICP-AES was used for the determination of the elements (Ca, Cr, K, Mg, Na, and P) and controlled with Intel Pentium IV PC and Liberty ICP-Expert Sequential (version: v.30) software. Each measurement was repeated three times ($n = 3$) and then standard errors of the means were calculated. The pH values of the metal solutions were measured with Consort-C864 (Belgium) multi-pH-meter. Ion chromatography (Shimadzu, Japan) was used to define NO_3^- within the metal solutions. The equipment was calibrated using Shimadzu anion (P/N 228-33603-93) standard solution prepared at different concentrations.

$Pb(NO_3)_2$ (Acros, ≥98.0%) were used for preparing the metal solutions. The pH of the metal solutions was adjusted with 0.1 M HNO_3 and 0.01 M NaOH. HNO_3 (Merck, 65%), NaOH (Merck, ≥97.0%), and NaCl (Merck, ≥99.5%) were used for the experiments.

2.3. Adsorption Experiments. Adsorption studies were performed in 100 mL Erlenmeyer flasks containing 0.4 g bone sorbent and 100 mL aqueous Pb (II) solutions, solid to liquid ratio 1 : 250, at a fixed temperature and a stirring rate of 200 rpm for 30 hours. The temperature was controlled by a water bath consisting of a glass beaker in a magnetic stirrer heater. Dried fish bones (B) were exposed to aqueous metal ions in order to determine their adsorption capacity values. The amount of Pb (II) (final metal concentration) was determined in the remaining metal solutions after filtration through a 0.45 μm Whatman filter by ICP-AES. All adsorption experiments were repeated three times ($n = 3$) and the standard errors of the means were calculated. B was used in the adsorption experiments of Pb (II). The effect of the initial concentration of the metal ions, pH, contact time, and temperature on the adsorption of Pb (II) onto B was investigated.

The adsorption capacities of fish bone as milligram per gram of bone (mg/g fish bone) were calculated with as follows [23]:

$$q_{e.\,\mathrm{exp}} = (C_0 - C_t) \cdot \frac{V}{W}, \tag{1}$$

where C_0 is the initial concentration of metal ions (mg/L) and C_t is the metal ion concentration after adsorption time t(mg/L). V is the volume of metal ion solutions (mL) and W is the weight of bone (g). $q_{e.\,\mathrm{exp}}$ and $q_{e,\mathrm{cal}}$ are the experimental and calculated adsorption capacities (mg/g).

3. Results and Discussion

3.1. Characterization of Sorbents. The elemental composition of B and B-Pb was determined by Carbon-Sulfur analyzer, ICP-AES, XRD, and SEM-EDX. The carbon, calcium, phosphorus, sodium, magnesium, and sulphur amounts (wt %) of B were found to be 10.65%, 28.72%, 13.58%, 0.93%, 0.51%, and 0.04% by ICP-AES and Carbon-Sulfur analyzer, respectively. Ca/P mole ratio of B was calculated as 1.63 according to the results of previous study [20]. Figure 1 shows the XRD analysis spectrum of B. XRD patterns of bone sorbent prepared in the present study agreed with the reference patterns of calcium phosphate ($Ca_2P_2O_7$, Ref. Code, 00-003-0605). Table 1 gives some physical results of surface analysis of B as surface area (m^2/g), pore volume (cm^3/g), and average pore width (Å). The analysis of surface area is useful in determining the surface details of the sorbent. The specific surface area of B was determined with the BET method by using nitrogen. Single point surface area of B was found to be 27.72 m^2/g. BJH pore volume, BET, and BJH pore widthwere determined as $2,83 \times 10^{-2}$ cm^3/g, 26.58, and 43.58 Å, respectively.

The FT-IR analysis of B and B-Pb is given in Figure 2. The bands at 3300 cm^{-1} are assigned to –OH stretching. The peaks at 1020 cm^{-1}, 963 cm^{-1}, 600 cm^{-1}, and 558 cm^{-1} are assigned to vibrations of $-PO_4^{-3}$ groups. The stretching and bending modes of $-CO_3^{-2}$ groups were attributed to peaks at 1413 cm^{-1} and 872 cm^{-1}. The $-CO_3^{-2}$ and $-PO_4^{-3}$ band intensities of B at 1413 cm^{-1} and 1020 cm^{-1} reduced when the Pb (II) was adsorbed onto its surface (Figure 2). It could be said that the adsorption of Pb ions from aqueous solutions the surfaces of bone sorbents were changed to vibrations of $-CO_3^{-2}$ and $-PO_4^{-3}$ groups.

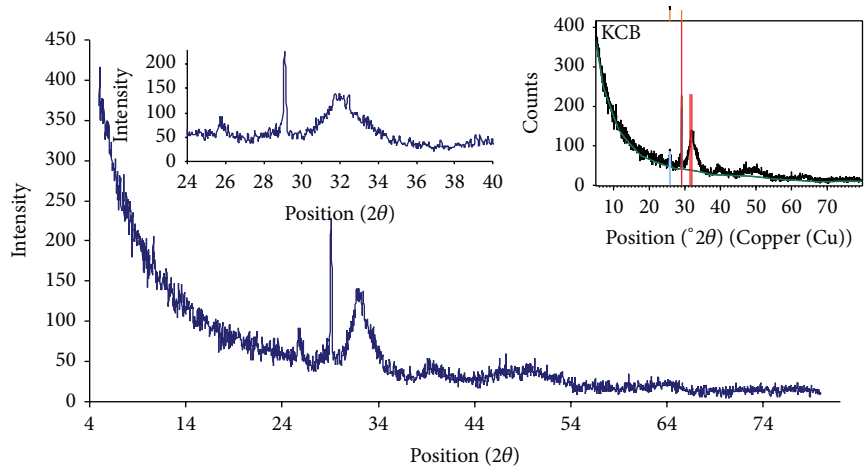

Figure 1: XRD spectra of B.

Table 1: Some physical results of BET surface analysis of pretreated fish bone.

Surface Area (m^2/g)	BET	Langmiur	SPSA[1]	t-Plot	BJH[2]
	13.45	101.60	27.72	28.06	25.97
Pore Volume (cm^3/g)	SPAV[3]		t-plot microvolume		BJH[4]
	8.94×10^{-3}		7.0×10^{-5}		2.83×10^{-2}
Average Pore Width (Å)	BET (4V/A)		BJH (4V/A)		
	26.58		43.58		

SPSA[1]: single point surface area at p/p°.
BJH[2]: BJH adsorption cumulative surface area of pores between 17.000 Å and 3000.000 Å width.
SPAV[3]: single point adsorption total pore volume of pores less than 14.767 Å width at p/p°.
BJH[4]: BJH adsorption cumulative volume of pores between 17.000 Å and 3000.000 Å width.

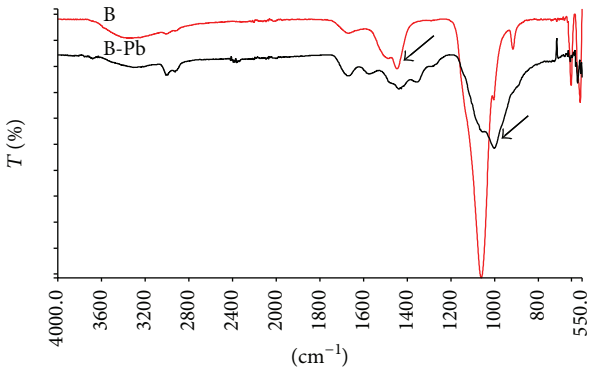

Figure 2: FT-IR spectra of B and B-Pb.

The adsorption of Pb^{2+} ions on to the fish bone surfaces can be explained with two different mechanisms. In the first adsorption mechanism, an ion exchange reaction occurred between metal ions in solution and Ca^{2+} ions of HAP on the bone surface [20, 24, 25]. This main removal mechanism is as the following reaction (*a*):

$$\mathrm{HAP} - \mathrm{Ca}_{10} \cdot (\mathrm{PO}_4)_6 \cdot (\mathrm{OH})_{2(\mathrm{Surface})} + x\mathrm{Pb}^{2+} + 2x\mathrm{NO}_3^- \longrightarrow \mathrm{Ca}_{(10-x)} \cdot \mathrm{Pb}_x \cdot (\mathrm{PO}_4)_6(\mathrm{OH})_2 + x\mathrm{Ca}^{2+} + 2x\mathrm{NO}_3^- \quad (a)$$

On the other hand, the second adsorption mechanism (*b*) took place between metal ions and Na^+ ions of HAP which was formed to HAP-(ONa) due to the alkali cleaning procedure (with NaOH solution) of the bone surface (*c*) [20]. These reactions (*b*) and (*c*) are given below:

$$(\mathrm{HAP} - \mathrm{ONa})_2^+ + x\mathrm{Pb}^{2+} + 2x\mathrm{NO}_{3\mathrm{aq}}^- \longrightarrow (\mathrm{HAP\text{-}O)\text{-}Pb\text{-}(O\text{-}HAP)} + x\mathrm{Ca}^{2+} + 2x\mathrm{NO}_3^- \quad (b)$$

$$\mathrm{Ca}_{10}(\mathrm{PO}_4)_6(\mathrm{OH})_{2(\mathrm{Surface})} + 2\mathrm{Na}^+ + 2\mathrm{OH}^- \longrightarrow \mathrm{Ca}_{10}(\mathrm{PO}_4)_6(\mathrm{ONa})_2 + 2\mathrm{H}_2\mathrm{O} \quad (c)$$

The initial concentration of NO_3^- ions in the solutions was not changed by the ion exchange reaction between metal ions and Ca^{2+} ions on the bone surface.

Table 2 and Figure 3 show the SEM-EDX analysis of B and B-Pb. The calcium percentages for B and B-Pb were found to be 36.44% and 14.63% and the Ca/P mole ratios of B and B-Pb were calculated as 1.60 and 1.06, respectively. The results in Figure 3 and Table 1 verified the Pb (II) adsorption on the bone surface by ion-exchange with calcium. Scanning electron microscope (SEM) images are useful in determining the surface and adsorption details of the bone sorbent during the adsorption [20]. The SEM images (Figure 4) show that the surfaces of B are slick and smooth. The surfaces of B-Pb exhibited roughness compared to the surfaces of B_{BBB}.

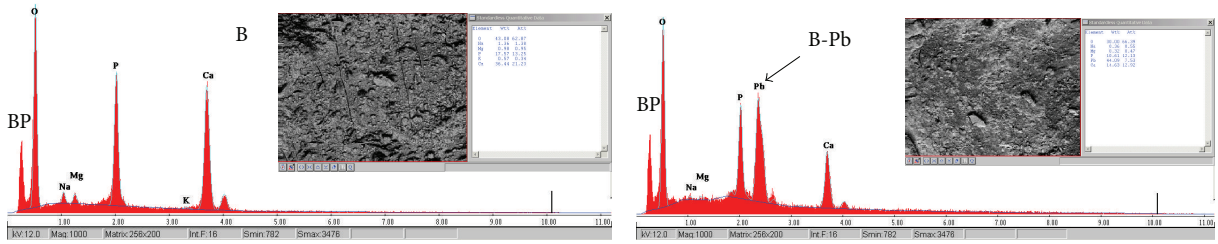

(a) (b)

Figure 3: SEM-EDX spectrum of (a) B and (b) B-Pb.

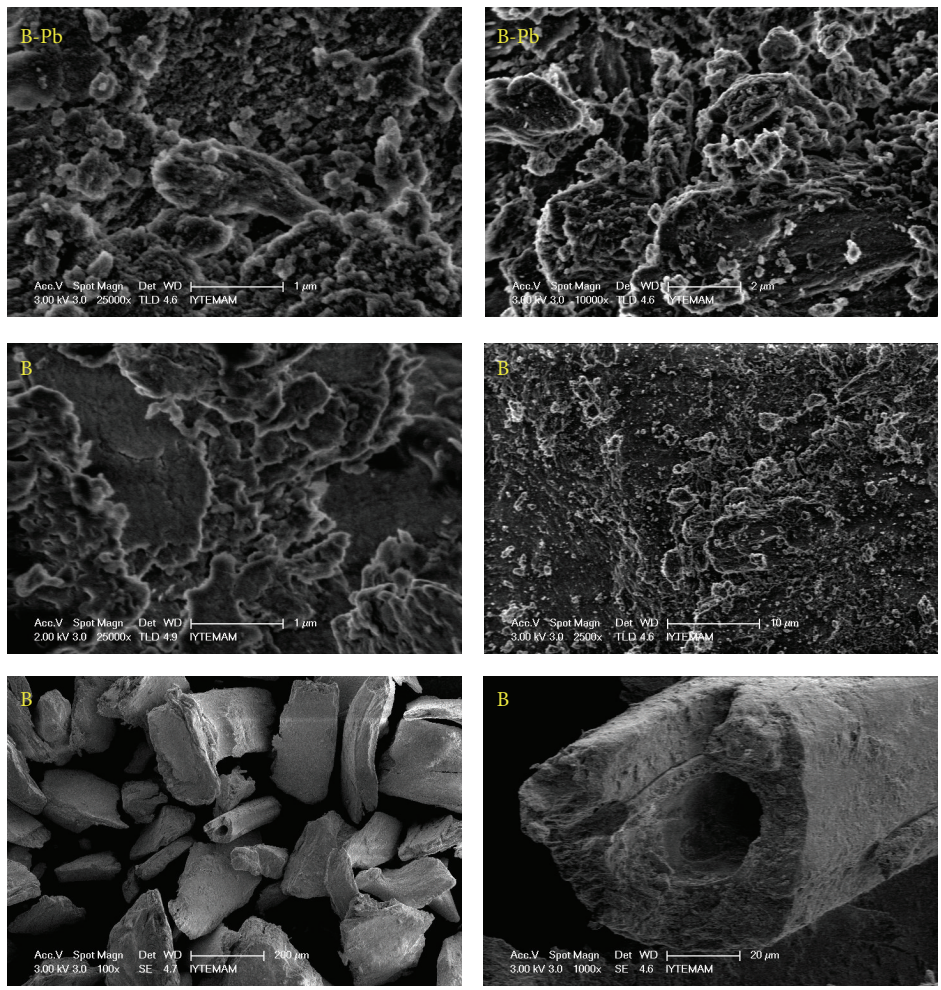

Figure 4: SEM images (1-2 μm) of (a) B-Pb and B.

SEM images of B-Pb clearly show that the bone surfaces with adsorbed Pb (II) are rough compared with surfaces of B. After the adsorption of metal ions from the aqueous solutions the surfaces of bone sorbents were changed. The change in the surfaces could be explained by the reaction (*b*). Based on this reaction, it could be said that very small HAP particles (<1 μm) were attached to the surfaces of bone sorbents by ion exchange between trivalent Pb metal ions and –ONa of HAP [20].

The DTA/TG analysis of B and B-Pb is shown in Table 3. The DTA/TGA analysis shows that B and B-Pb have 69.88% and 74.55% inorganic residue amount (RA) with mono weight losses at 800°C, respectively. The weight losses of 10% for B and B-Pb were found to be 328°C and 336°C,

Table 2: Element compositions and Ca/P mole ratios of fish bones by SEM-EDX.

Element (wt%)	Ca	P	Na	Mg	K	O	Pb	Ca/P	Total wt%
B	36.44	17.57	1.36	0.98	0.57	43.08	—	1.60	100
*B-Pb	14.63	10.61	0.36	0.32	—	30.00	44.09	1.06	100

*Adsorbed Pb of the B_{BBB} sorbent.

Table 3: DTA/TG results of B and B-Pb.

	TGA					DTA	
	D_1 (°C)	D_2 (°C)	D_3 (25%) (°C)	D_4 (10%) (°C)	RA (wt%) at 800°C	Exo.	Endo.
B	211	352	508	328	69.88	392	—
B-Pb	207	354	775	336	74.55	390	—

D_1: the starting temperature of degradation; D_2: maximum degradation temperature; D_3 and D_4: weight losses with 25 and 10 wt%; RA: residue amount (wt%); Exo.: exothermic; Endo.: endothermic.

respectively. The maximum degradation temperatures (D_2) of B and B-Pb were calculated as 352°C and 354°C, respectively.

3.2. Effect of pH. The effect of pH on the adsorption of Pb (II) on the pretreated fish bones B was studied in the pH range of 3 and 5.5 at 780 mg/L of initial metal concentration. The initial pH values were adjusted by adding diluted HNO_3 and NaOH solutions. The results are shown in Figure 5 and Table 4. Since HAP, the main constituent of the fish bones, starts to dissolve at pH lower than 3, the initial pH was chosen to be 3 [11]. The pH values higher than 5.5 were not studied because the precipitation of lead ions as lead hydroxides occurs at high concentrations [26]. In this study, a number of kinetic, temperature, pH, and time experiments were carried out on high lead concentrations (like 2000 mg/L lead (II) solutions) and therefore, the selected pH value of 5 was chosen in order to prevent the formation of lead hydroxides and to get comparable results at standard pH. pH 5 was selected instead of pH 3, because this pH is close to natural water.

Figure 5 demonstrates that the adsorption capacity for Pb (II) increased with increasing pH. The highest adsorption capacity was found to be 118.7 mg/g at pH 5.5 and the results of lead removal capacities at different pH values are given in Table 4. The effect of pH plays an important role in the phosphate and hydroxyl groups of HAP during the cation-exchange reaction on the bone surface. At lower pH, HAP is dissolved and protons compete with metal ions for a binding site. The concentration of protons at lower pH is higher; thus, more groups are bound with protons and therefore fewer groups are available for metal ions to bind with [27].

3.3. Kinetic Study. The modeling of the kinetics of adsorption of Pb (II) using B_{BBB} was investigated by using two common models: pseudo-first and second-order kinetic equations. The Lagergren equation was used for the pseudo-first-order equation (2) [28, 29]:

$$\ln\left(q_e - q_t\right) = \ln q_{e,\mathrm{cal}} - k_1 \cdot t, \tag{2}$$

where k_1 is the rate constant of pseudo-first-order sorption (h^{-1}) and q_e and q_t are the amounts of metal adsorbed per gram of fish bone (mg/g bone) at equilibrium and any time, respectively. The plot of $\ln(q_e - q_t)$ versus t for pseudo-first-order kinetics showed a linear relationship. The slope and intercept of $\ln(q_e - q_t)$ versus t were used to calculate the pseudo-first-order rate constant k_1 and $q_{e,\mathrm{cal}}$, shown in Table 5. Equation (3) was used for the pseudo-second-order kinetic model [30, 31]:

$$\frac{t}{q_t} = \frac{1}{k_2 {q_{e,\mathrm{cal}}}^2} + \frac{t}{q_{e,\mathrm{cal}}}, \tag{3}$$

where k_2 (g bone/mg hour) is the rate constant for pseudo-second-order adsorption. The constants $q_{e,\mathrm{cal}}$ and k_2 values were calculated from the slopes and intercepts of t/q_t versus t plots. h_i value was calculated using k_2 rate constant obtained from pseudo-second-order kinetic data and expressed as

$$h_i = k_2 q_{e,\mathrm{cal}}^2, \tag{4}$$

where the value of h_i is the initial metal adsorption rate (mg/g bone hour) [32]. The constants k_2, $q_{e,\mathrm{cal}}$, and h were calculated from the intercept and slope of the line obtained by plotting t/q_t against t and are shown in Table 5.

The kinetic data obtained from Pb (II) adsorption experiments were analyzed using the pseudo-first-order kinetic model according to (2) and the results are given in Table 5. Maximum rate constants k_1 were determined at a temperature of 30°C. The calculated adsorption values ($q_{e,\mathrm{cal}}$) are not supported by the experimental data ($q_{e,\mathrm{cal}}$). The highest k_2 values at different temperatures and concentrations were found to be 2.13 g/mg·h and 3.76×10^{-3} g/mg·h at 50°C and 417 mg/L, respectively. The effect of time on the adsorption capacity for Pb (II) at different temperatures is given in Figure 6.

According to Table 5, the correlation coefficients (R^2) of the pseudo-second-order kinetic model for the linear plots are higher than 0.99 for all the temperatures and concentrations. On the other hand, when R values of the pseudo-second-order kinetic model are calculated from the R^2 values, it is clearly shown that R values for all the temperatures and concentrations are higher than 0.9999 and at the same time are higher than the R values of the pseudo-first-order kinetic model. The calculated ($q_{e,\mathrm{cal}}$) adsorption amount for the pseudo second-order kinetic model is close to

Table 4: Results of lead removal capacities at different pHs.

782 mg Pb^{+2}/L 20°C	pH			
	3	4	5	5.5
$q_{e,exp}$ (mg/g) ± SEM*	112.36 ± 2.13	116.00 ± 1.98	117.45 ± 1.92	118.79 ± 1.90
% Removal	57.43	59.29	60.03	60.72

*SEM: standard error of the means ($n = 3$).

Table 5: Pseudo-first and second-order kinetic constants of Pb (II) at different temperatures and concentrations.

		Pseudo-first-order			Pseudo-second-order			
	$q_{e,exp}$ (mg/g)	$q_{e,theo}$ (mg/g)	k_1 (h^{-1})	R^2	$q_{e,theo}$ (mg/g)	k_2 (g/mg·h)	h_i (mg/g·h)	R^2
pH 5, 1667 mg Pb^{+2}/L								
20°C	153.37	135.08	0.175	0.994	170.25	1.87×10^{-3}	54.08	0.998
30°C	216.32	185.78	0.220	0.979	234.66	1.91×10^{-3}	105.35	0.998
40°C	267.93	200.81	0.214	0.986	285.31	2.02×10^{-3}	164.71	0.999
50°C	323.21	214.99	0.216	0.981	339.95	2.13×10^{-3}	246.18	0.999
pH 5, 20°C								
50 mg/L	12.56	11.64	0.188	0.974	13.55	2.87×10^{-2}	5.26	0.995
417 mg/L	86.05	76.41	0.208	0.996	95.45	3.76×10^{-3}	34.22	0.999
782 mg/L	117.45	114.08	0.201	0.980	129.92	2.56×10^{-3}	43.19	0.995
1667 mg/L	153.37	135.08	0.175	0.994	170.25	1.87×10^{-3}	54.08	0.998

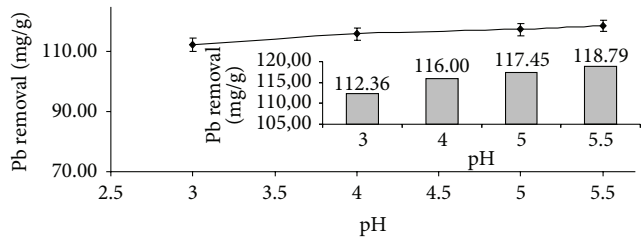

Figure 5: The effect of pH on the adsorption of Pb.

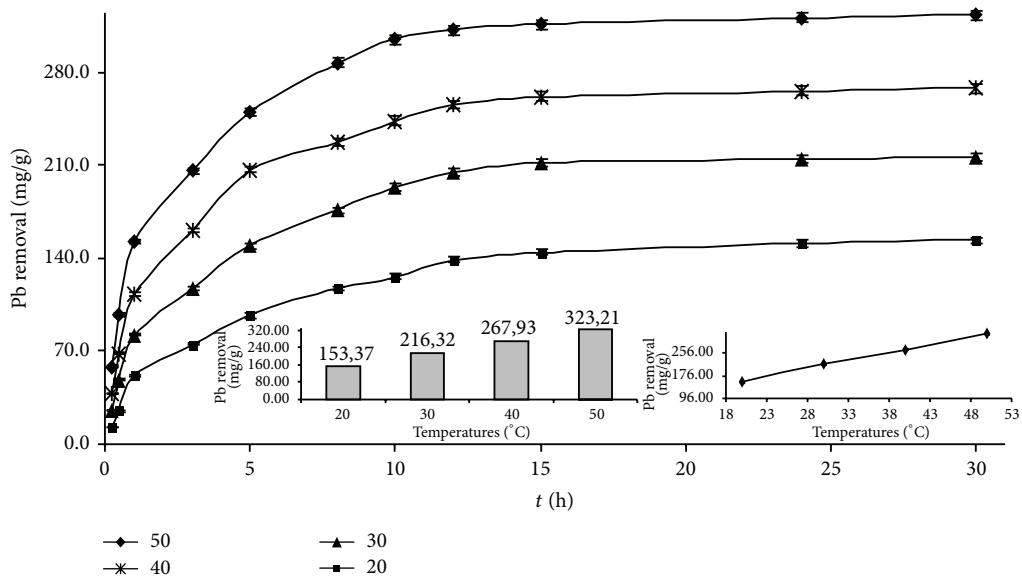

Figure 6: The effect of contact time and temperature on the adsorption of Pb (II).

Table 6: Diffusion constants of Pb (II) at different temperatures and concentrations.

	Urano and Tachikawa		Weber and Morris			
	D_i (m^2h^{-1})	R^2	K_w ($mg\,g^{-1}h^{-0.5}$)	C (mg/g)	D_w (m^2h^{-1})	R^2
pH 5, 1667 mg Pb^{+2}/L						
20°C	2.61×10^{-11}	0.991	38.93	3.32	2.34×10^{-13}	0.979
30°C	5.00×10^{-11}	0.974	55.06	15.13	2.35×10^{-13}	0.976
40°C	4.88×10^{-11}	0.990	65.83	32.47	2.19×10^{-13}	0.951
50°C	4.98×10^{-11}	0.990	75.73	56.45	1.99×10^{-13}	0.943
pH 5, 20°C						
50 mg/L	4.19×10^{-11}	0.949	2.87	1.19	1.89×10^{-13}	0.962
417 mg/L	4.66×10^{-11}	0.991	23.13	1.60	2.62×10^{-13}	0.962
782 mg/L	4.47×10^{-11}	0.962	29.56	3.23	2.30×10^{-13}	0.993
1667 mg/L	2.61×10^{-11}	0.991	38.93	3.32	2.34×10^{-13}	0.979

the experimental data ($q_{e,\text{exp}}$), but $q_{e,\text{cal}}$ for the pseudo-first-order kinetic model are generally not supported by $q_{e,\text{exp}}$. The correlation coefficients of the pseudo-second-order kinetic model for the linear plots are higher than 0.99 for all the temperatures and concentrations. According to the correlation coefficient constant (R^2) and the experimental adsorption amount ($q_{e,\text{exp}}$), it could be said that the experimental data exhibit a good compliance with the pseudo second-order equation for Pb (II) removal. Similar kinetic applications were also determined for Co (II) removal with animal bone [11], in which the adsorption rate of Co (II) ions on the animal bones was described by a second-order rate expression; the pseudo-second-order model correlates well with the experimental data on the sorption of divalent and trivalent metal cations by synthetic HAP [33].

3.4. Diffusion Parameters. The intraparticle diffusion model (IPD) of Weber and Morris has been widely applied to the analysis of adsorption kinetics [34]. Weber-Morris and Urano-Tachikawa modeling were used to model the diffusion of Pb (II) from aqueous solution using B_{BBB}.

The Weber and Morris diffusion model is expressed as [15, 35, 36]

$$q_t = Kw \cdot t^{0.5} + C. \tag{5}$$

In this equation, Kw ($mg \cdot g^{-1}h^{-0.5}$) is the Weber and Morris intraparticle diffusion rate constant and C is a value of intercept constant of the plot that provide information about thickness of the boundary layer (mg/g). The value of q_t (the amount of adsorption at any time) is plotted against $t^{0.5}$ (the square root of time) to get a straight line. The intraparticle diffusion constant (Kw) was calculated from the slopes of q_t versus $t^{0.5}$ plots.

The intraparticle diffusion coefficient (Dw) was calculated using [37, 38]

$$Dw = \left(\frac{\pi}{8640}\right)\left(\frac{dKw}{q_e}\right)^2, \tag{6}$$

where Dw (m^2h^{-1}) is the diffusion coefficient in the solid and d (m) is the mean particle diameter.

The following equation (7) was used for the intraparticle diffusion model of Urano and Tachikawa [37, 39]:

$$-\log\left[1-\left(\frac{q_t}{q_e}\right)^2\right] = 4\pi^2\frac{D_i t}{2.3d^2}, \tag{7}$$

where D_i was calculated from the slopes of $-\log[1-(q/q_e)^2]$ versus t plots.

The values of Kw, Dw, D_i, and C are given in Table 6. The highest D_i values for the Urano and Tachikawa model were found to be $5.00\,m^2\,h^{-1}$ at 30°C. The maximum Kw values according to the Weber and Morris model were found to be $75.7\,mg\,g^{-1}\,h^{-0.5}$ at 50°C. The constant C increased with the increase in temperature from 20°C to 50°C and likewise increased with the increase in concentration. The value of the intercepts of the plot of $t^{0.5}$ versus q_e and the constant C from (5) provide information about the boundary layer effect for the Weber and Morris model. An increase in the value of constant C indicates the abundance of solute adsorbed by the boundary effect [36]. Our results were similar to the research of Bilgili [40], who reported that Kw values decreased and C values increased with increasing temperatures. Dw was found to decrease from $2.34\,m^2h^{-1}$ to $1.99 \times 10^{-13}\,m^2h^{-1}$ with an increase in temperature from 20°C to 50°C except for at 30°C, respectively. On the other hand, Dw was found to increase from $1.89\,m^2h^{-1}$ to $2.34 \times 10^{-13}\,m^2h^{-1}$ with an increase in concentration from 50 mg/L to 1667 mg/L except for at 417 mg/L, respectively. According to Greluk and Hubicki [36], if the intraparticle diffusion Kw is involved in the adsorption process, then the plot of $t^{0.5}$ versus q_e would result in a linear graph and the process of intraparticle diffusion would be the controlling step if this line passed through the origin. When the data exhibit multilinear plots which do not pass through the origin, this is indicative of some degree of boundary layer control and further shows that intraparticle diffusion is not the only rate-controlling factor, but that other processes may control the rate of sorption [36].

Table 7: Results of removal capacities at different temperatures and thermodynamic constants of Pb (II).

pH 5, 1667 mg Pb^{+2}/L	Temperatures (°C)				
	20	30	40		50
$q_{e,exp}$ (mg/g) ± SEM*	153.37 ± 2.53	216.32 ± 2.90	267.93 ± 3.24		323.21 ± 3.65
% Removal	36.80	51.90	64.29		77.55
ΔH° (KJ mol^{-1})	ΔS° (KJ $mol^{-1}K^{-1}$)	ΔG° (KJ mol^{-1})			E_a (KJ mol^{-1})
		20°C	30°C	40°C	50°C	
46.01	0.141	4.73	3.32	1.91	0.50	7.06

*SEM: standard error of the means ($n = 3$).

The values of D_i and Dw are different from each other and the Weber and Morris model gives lower diffusion coefficients than the Urano and Tachikawa model. Generally, Table 6 shows that R^2 values and intraparticle diffusion of the Urano and Tachikawa model were better than those of the Weber and Morris model. Thus, it can be concluded that the experimental data for the intraparticle diffusion model of Pb (II) on the bone sorbents fit the Urano and Tachikawa model.

3.5. Temperatures and Thermodynamic Parameters. The activation energy (E_a) for the adsorption of Pb (II) was determined using the Arrhenius equation and is expressed as [29]

$$\ln k = \ln A - \frac{E_a}{RT}, \tag{8}$$

where k is the rate constant k_2 (pseudo-second-order) which was obtained from Table 3, E_a (kJ mol^{-1}), T(K), R (kJ mol^{-1} K^{-1}), and A are the Arrhenius activation energy, temperature of the adsorption medium, the gas constant and the Arrhenius factor, respectively. The activation energy E_a was calculated from the slope of the line obtained by plotting $\ln k$ against $1/T$ and is shown in Table 4.

The thermodynamic parameters known as Gibbs free energy (ΔG°), enthalpy (ΔH°), and entropy (ΔS°) were determined by using the following equations [32, 41–43]:

$$K_c = \frac{C_a}{C_e} \tag{9}$$

$$\Delta G^\circ = \Delta H^\circ - T\Delta S^\circ \tag{10}$$

$$\ln K_c = \frac{\Delta S^\circ}{R} - \frac{\Delta H^\circ}{RT}, \tag{11}$$

where C_a and C_e are the amount of metal ions (mg) adsorbed on the adsorbent per liter of the solution at equilibrium time and the equilibrium concentration (mg/L) of metal ions in the solution, respectively. The K_c value is used in (11) to determine the thermodynamic parameters of adsorption. $T(K)$ and R are the solution temperature and gas constant, respectively. The constants of $\Delta H^\circ$and ΔS° were calculated from the slope and intercept of van't Hoff plots of $\ln K_c$ versus $1/T$. The free energy (ΔG°) was calculated from (10) using ΔH° and ΔS°. The results are shown in Table 4. The Gibbs free energy indicates the fundamental of spontaneity of the adsorption process. When ΔG° is a negative quantity, the adsorption process occurs spontaneously and higher negative values reflect a more energetically favorable adsorption [42].

The values of E_a, ΔH°, and ΔS° were found to be 7.06, 46.01 kJ mol^{-1}, and 0.141 kJ $mol^{-1}K^{-1}$ for Pb (III), respectively (Table 7). The values of ΔG° for the temperatures of 20°C, 30°C, 40°C, and 50°C were found to be 4.73 kJ mol^{-1}, 3.32 kJ mol^{-1}, 1.91 kJ mol^{-1}, and 0.50 kJ mol^{-1}, respectively. According to Şeker et al. [30], if the value of E_a is between 8.4 kJ mol^{-1} and 83.7 kJ mol^{-1}, the adsorption is said to be chemical type and the rate constant changes with temperature according to the activation energy in the Arrhenius equation (8). The positive values of ΔG° at temperatures lower than 55°C (328 K) show that the adsorption of Pb (II) ions onto the fish bonesis nonspontaneous; in other words the adsorption process requires higher temperatures to occur. It could be explained that the ion exchange amounts of metal ions with calcium at the solid/liquid interface at low temperatures are lower than those at higher temperatures during the sorbates and sorbents interaction. When the temperature increased beyond 328 K (55°C), the ΔG° values turned to negative. For example, the ΔG° for 328 K (55°C) is calculated as −0.238 kJ/mol. According to Lazarević et al. [44], this state points the presence of an energy barrier for the sorption process. The positive values of Gibbs free energy (ΔG°) indicate that the adsorption process requires a small amount of energy with increasing temperature [44]. On the other hand, according to Zhou et al. [23], the decrease in ΔG° with increasing temperature implies a greater driving force and more spontaneous adsorption at high temperature. Similar calculations of thermodynamic parameters were also determined for Ni (II) removal with Sepiolite by Lazarević et al. [44]. According to Lazarević et al. [44], enthalpy (ΔH°) and entropy (ΔS°) for Ni (II) removal with sepiolite were found to be 27.93 kJ/mol and 0.0767 kJ/mol K, respectively, and the Gibbs free energy (ΔG°) was found to decrease from 5.05 kJ/mol at 25°C to 1.98 kJ/mol at 65°C. For the positive ΔG°, Lazarević et al. [44] have explained that "Considering the positive values of ΔG°, it has been suggested that this is quite common for the sorption of metal ions by the ion exchange mechanism, because an activated complex of a metal ion is formed with the sorbent in the excited state." On the other hand, the values of ΔH° ΔS° and ΔG° in the study of Gupta et al. [45] were found to be 4.519 kJ/mol, 0.0491 kJ/mol K and 4.519 519 kJ/mol, respectively. In the studies of Guan et al. [46] and Bhaumik et al. [47] show that all values of ΔH°, ΔS°, and ΔG° were determined as positive. The positive values

Table 8: Removal capacities and adsorption isotherms constants of Pb (II) at different initial concentrations.

pH 5, 20°C	Initial concentration (mg/L)						
	50.92	240.81	417.46	782.52	1042.55	1667.09	2036.26
$q_{e,exp}$ (mg/g) ± SEM*	12.56 ± 0.20	59.82 ± 0.23	86.05 ± 1.53	117.45 ± 1.92	129.98 ± 2.22	153.37 ± 2.46	155.66 ± 2.53
% Removal	98.66	99.35	82.45	60.03	49.87	36.80	30.58
	Freundlich			Langmuir			
K_F	n	R^2		Q_{max} (mg/g)	b (L/mg)	R^2	R_L
26.54	3.90	0.806		158.51	2.03×10^{-3}	0.993	0.906

*SEM: standard error of the means ($n = 3$).

of enthalpy (ΔH°) show that the adsorption and removal of metal ions using bone sorbents are the endothermic case and the positive Gibbs' free energy (ΔG°) values confirm that the adsorption process for Pb (II) ions requires heat to proceed. Entropy has been defined as the degree of randomness of systems and ΔS° for Pb was found to be a positive value in our study. The positive values of entropy may be a result of some structural changes in the bone sorbent which result in increased electronegativity and decreased atomic volume (for Pb) during the adsorption process between the metal and Ca^{2+} ions. The adsorption capacities at different temperatures are given in Table 7. The highest removal was found to be 323.2 mg/g at 50°C.

3.6. Adsorption Isotherms. Adsorption isotherms are widely used as important criteria in optimizing the use of adsorbents because they describe the nature ofthe interaction between adsorbate and adsorbent [17]. Two isotherms were used to describe the experimental results for the adsorption process of Pb (II) ions on fish bone, namely, the Langmuir and the Freundlich adsorption isotherms.

The Langmuir adsorption model assumes that the adsorbent surface has a saturated monolayer of molecules and finite number of identical sites which shows homogeneous surfaces [48]. The Langmuir equation is given by [49, 50]

$$\frac{C_e}{q_e} = \frac{C_e}{Q_{max}} + \frac{1}{Q_{max} b}, \tag{12}$$

where C_e (mg/L) and q_e (mg/g) are the residual metal concentration in solution and the amount of the metal adsorbed on the sorbent at equilibrium, respectively. Q_{max} (mg/g) is the maximum amount of the metal ions per unit weight of sorbent and b is the Langmuir adsorption equilibrium constant related to the affinity between the sorbent and metal ions. For the calculation of the Langmuir adsorption equilibrium constant, the plot of (C_e/q_e) versus C_e showed a linear relationship. The constants Q_{max} and b were calculated from the slope and intercept of the curve of (C_e/q_e) versus C_e and the obtained results are shown in Table 8.

To determine whether the adsorption process was favourable or unfavourable for the Langmuir adsorption, R_L was used, given in [23, 51, 52]

$$R_L = \frac{1}{(1 + bC_0)}, \tag{13}$$

where C_0 (mg/L) and b (L/mg) are initial metal concentration and Langmuir constant, respectively. The value of R_L indicates the shape of the isotherm to be unfavorable ($R_L > 1$), linear ($R_L = 1$), favorable ($0 < R_L < 1$), or irreversible ($R_L = 0$). The R_L values between 0 and 1 indicate favorable adsorption [35].

The Freundlich equation is applicable to heterogeneous surfaces and multilayer adsorption [48]. The linear form of the Freundlich equation is given by following equation [53, 54]:

$$\ln q_e = \ln K_F + \left(\frac{1}{n}\right) \ln C_e, \tag{14}$$

where K_F and n are the adsorption capacity of the sorbent and adsorption intensity, respectively. For calculation of Freundlich adsorption equilibrium constants, the plot of $\ln q_e$ versus $\ln C_e$ shows a linear relationship. The values of K_F and n are calculated from the intercept and slope of the plot of $\ln q_e$ versus $\ln C_e$ and the results are given in Table 8.

The adsorption amounts depending on concentrations are shown in Figure 7. The constants K_F, n, and R^2 obtained from the Freundlich isotherm were found to be 26.5, 3.9, and 0.806, respectively. Based on the calculated correlation coefficients (R^2) for the Langmuir and Freundlich isotherms, it can be suggested that the experimental data for the adsorption of Pb (II) on the bones fit the Langmuir isotherm model. The value of R_L was found to be 0.906 (Table 8). The calculated R_L value indicated that the adsorption of Pb (II) ions on the fish bones was favorable Pb (II) concentration. The adsorption capacities at different concentrations are given in Table 8. The highest removal was found to be 155.6 at 2036 mg/L. The lead removal capacities of various adsorbents given in the literature are summarized in Table 9. Table 9 clearly shows that pretreated fish bones appear to be very useful sorbent.

4. Conclusion

Fish bones, one of the most abundant fish-processing industry waste products, were investigated for lead removal. With many specific advantages such as low cost, easy availability, natural origin, and high adsorption capacity, fish waste products can be used as sorbents to remove heavy metal. In this study, fish bones which exhibited high sorption capacity were used as a natural sorbent to remove lead.

The highest removal capacity for Pb (II) was found to be 323 mg/g at 50°C. The experiments showed that when pH

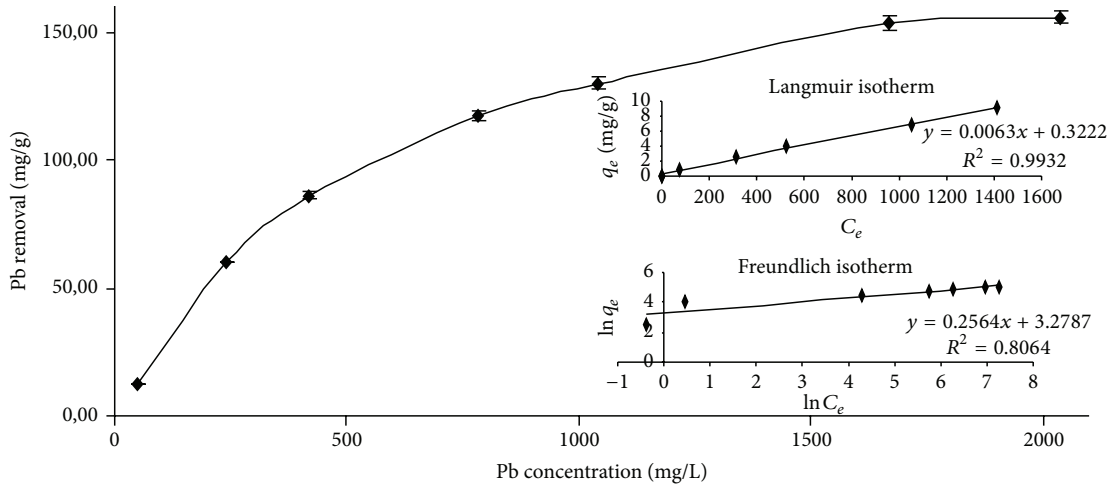

Figure 7: The effect of concentration on the adsorption of Pb (II).

Table 9: Comparison of lead removal with different adsorbents.

Adsorbents	Removal capacity (mg/g)	Reference
Pretreated fish bones	323.21	This study
Seaweed (*Gymnogongrus Torulosus*)	140.89	[17]
Algal biomass (*Oedogonium* sp. and *Nostoc* sp.)	145.0	[19]
Fruit shell (Mangostana)	3.56	[55]
Water hyacinth weed	26.32	[56]
Peels of banana	2.18	[57]
Saccharomyces cerevisiae biomass	83.33	[58]

increased, an increase in the adsorption capacity of the fish bones was observed. The correlation coefficients showed that the experimental data for the adsorption of Pb fitted well to the Langmuir isotherm model and the value of R_L for Pb (II) was found to be 0.906. The kinetic data fitted a pseudo-second-order kinetic model. The enthalpy ΔH° of lead was calculated as 46.01 kJ mol^{-1} and the adsorption mechanism was endothermic. The activation energy, E_a of adsorption of Pb (II), was determined as 7.06 kJ/mol. The experimental results showed that the correlation coefficients of intraparticle diffusion of the Urano and Tachikawa model were better than those of the Weber and Morris model. Desorption/leaching experiments showed that desorption of the Pb on the bone surface exhibited very low ratios. Fish bones can be used as adsorbent with simple processing. Therefore, the utilization of pretreated fish bones could be low cost and effective and might contribute to the protection of the environment.

Conflict of Interests

The authors declare that there is no conflict of interests regarding the publication of this paper.

Acknowledgments

The authors acknowledge the Scientific Research Project Commission of Canakkale Onsekiz Mart University (Project no: 2010/16) for financial support. The authors wish to thank the Central Laboratory of Canakkale Onsekiz Mart University.

References

[1] H. Kalavathy, B. Karthik, and L. R. Miranda, "Removal and recovery of Ni and Zn from aqueous solution using activated carbon from *Hevea brasiliensis*: batch and column studies," *Colloids and Surfaces B: Biointerfaces*, vol. 78, no. 2, pp. 291–302, 2010.

[2] P. H. Kansanen and J. Venetvaara, "Comparison of biological collectors of airborne heavy metals near ferrochrome and steel works," *Water, Air, and Soil Pollution*, vol. 60, no. 3-4, pp. 337–359, 1991.

[3] E. Pip, "Cadmium, copper, and lead in soils and garden produce near a metal smelter at Flin Flon, Manitoba," *Bulletin of Environmental Contamination and Toxicology*, vol. 46, no. 5, pp. 790–796, 1991.

[4] H. Huang, G. Cheng, L. Chen, X. Zhu, and H. Xu, "Lead (II) removal from aqueous solution by spent agaricus bisporus: determination of optimum process condition using Taguchi method," *Water, Air, and Soil Pollution*, vol. 203, no. 1–4, pp. 53–63, 2009.

[5] A. S. Özcan, Ö. Gök, and A. Özcan, "Adsorption of lead(II) ions onto 8-hydroxy quinoline-immobilized bentonite," *Journal of Hazardous Materials*, vol. 161, no. 1, pp. 499–509, 2009.

[6] H. Ghassabzadeh, M. Torab-Mostaedi, A. Mohaddespour, M. G. Maragheh, S. J. Ahmadi, and P. Zaheri, "Characterizations of Co

(II) and Pb (II) removal process from aqueous solutions using expanded perlite," *Desalination*, vol. 261, no. 1-2, pp. 73–79, 2010.

[7] R. Donat, A. Akdogan, E. Erdem, and H. Cetisli, "Thermodynamics of Pb^{2+} and Ni^{2+} adsorption onto natural bentonite from aqueous solutions," *Journal of Colloid and Interface Science*, vol. 286, no. 1, pp. 43–52, 2005.

[8] S. E. Bailey, T. J. Olin, R. M. Bricka, and D. D. Adrian, "A review of potentially low-cost sorbents for heavy metals," *Water Research*, vol. 33, no. 11, pp. 2469–2479, 1999.

[9] A. Bhatnagar and A. K. Minocha, "Biosorption optimization of nickel removal from water using *Punica granatum* peel waste," *Colloids and Surfaces B: Biointerfaces*, vol. 76, no. 2, pp. 544–548, 2010.

[10] X.-F. Sun, C. Liu, Y. Ma, S.-G. Wang, B.-Y. Gao, and X.-M. Li, "Enhanced Cu(II) and Cr(VI) biosorption capacity on poly(ethylenimine) grafted aerobic granular sludge," *Colloids and Surfaces B: Biointerfaces*, vol. 82, no. 2, pp. 456–462, 2011.

[11] S. Dimovic, I. Smiciklas, I. Plećaš, D. Antonovic, and M. Mitric, "Comparative study of differently treated animal bones for Co^{2+} removal," *Journal of Hazardous Materials*, vol. 164, no. 1, pp. 279–287, 2009.

[12] F. Banat, S. Al-Asheh, and F. Mohai, "Batch zinc removal from aqueous solution using dried animal bones," *Separation and Purification Technology*, vol. 21, no. 1-2, pp. 155–164, 2000.

[13] Y. Zhang, Y. Liu, X. Ji, C. E. Banks, and J. Song, "Flower-like agglomerates of hydroxyapatite crystals formed on an egg-shell membrane," *Colloids and Surfaces B: Biointerfaces*, vol. 82, no. 2, pp. 490–496, 2011.

[14] S. S. Baral, S. N. Das, G. R. Chaudhury, and P. Rath, "Adsorption of Cr (VI) by treated weed *Salvinia cucullata*: kinetics and mechanism," *Adsorption*, vol. 14, no. 1, pp. 111–121, 2008.

[15] A. El-Sikaily, A. El Nemr, A. Khaled, and O. Abdelwehab, "Removal of toxic chromium from wastewater using green alga *Ulva lactuca* and its activated carbon," *Journal of Hazardous Materials*, vol. 148, no. 1-2, pp. 216–228, 2007.

[16] J. R. Memon, S. Q. Memon, M. I. Bhanger, A. El-Turki, K. R. Hallam, and G. C. Allen, "Banana peel: a green and economical sorbent for the selective removal of Cr(VI) from industrial wastewater," *Colloids and Surfaces B: Biointerfaces*, vol. 70, no. 2, pp. 232–237, 2009.

[17] M. M. Areco and M. D. S. Afonso, "Copper, zinc, cadmium and lead biosorption by *Gymnogongrus torulosus*. Thermodynamics and kinetics studies," *Colloids and Surfaces B: Biointerfaces*, vol. 81, no. 2, pp. 620–628, 2010.

[18] K. S. Rao, S. Anand, and P. Venkateswarlu, "Adsorption of cadmium from aqueous solution by *Ficus religiosa* leaf powder and characterization of loaded biosorbent," *CLEAN—Soil, Air, Water*, vol. 39, no. 4, pp. 384–391, 2011.

[19] M. Z. Alam and S. Ahmad, "Chromium removal through biosorption and bioaccumulation by bacteria from tannery effluents contaminated soil," *CLEAN—Soil, Air, Water*, vol. 39, no. 3, pp. 226–237, 2011.

[20] B. Kizilkaya, A. A. Tekinay, and Y. Dilgin, "Adsorption and removal of Cu (II) ions from aqueous solution using pretreated fish bones," *Desalination*, vol. 264, no. 1-2, pp. 37–47, 2010.

[21] M. Ozawa, K. Satake, and R. Suzuki, "Removal of aqueous chromium by fish bone waste originated hydroxyapatite," *Journal of Materials Science Letters*, vol. 22, no. 7, pp. 513–514, 2003.

[22] I. Smičiklas, S. Dimović, I. Plećaš, and M. Mitrić, "Removal of Co^{2+} from aqueous solutions by hydroxyapatite," *Water Research*, vol. 40, no. 12, pp. 2267–2274, 2006.

[23] Y.-T. Zhou, C. Branford-White, H.-L. Nie, and L.-M. Zhu, "Adsorption mechanism of Cu^{2+} from aqueous solution by chitosan-coated magnetic nanoparticles modified with α-ketoglutaric acid," *Colloids and Surfaces B: Biointerfaces*, vol. 74, no. 1, pp. 244–252, 2009.

[24] S. H. Jang, B. G. Min, Y. G. Jeong, W. S. Lyoo, and S. C. Lee, "Removal of lead ions in aqueous solution by hydroxyapatite/polyurethane composite foams," *Journal of Hazardous Materials*, vol. 152, no. 3, pp. 1285–1292, 2008.

[25] C. Stötzel, F. A. Müller, F. Reinert, F. Niederdraenk, J. E. Barralet, and U. Gbureck, "Ion adsorption behaviour of hydroxyapatite with different crystallinities," *Colloids and Surfaces B: Biointerfaces*, vol. 74, no. 1, pp. 91–95, 2009.

[26] I. Chaari, E. Fakhfakh, S. Chakroun et al., "Lead removal from aqueous solutions by a Tunisian smectitic clay," *Journal of Hazardous Materials*, vol. 156, no. 1–3, pp. 545–551, 2008.

[27] K. Chojnacka, "Biosorption of Cr(III) ions by eggshells," *Journal of Hazardous Materials*, vol. 121, no. 1–3, pp. 167–173, 2005.

[28] S. Chowdhury and P. Saha, "Adsorption kinetic modeling of safranin onto rice husk biomatrix using pseudo-first- and pseudo-second-order kinetic models: comparison of linear and non-linear methods," *CLEAN—Soil, Air, Water*, vol. 39, no. 3, pp. 274–282, 2011.

[29] Ç. Doğar, A. Gürses, M. Açıkyildiz, and E. Özkan, "Thermodynamics and kinetic studies of biosorption of a basic dye from aqueous solution using green algae *Ulothrix* sp.," *Colloids and Surfaces B: Biointerfaces*, vol. 76, no. 1, pp. 279–285, 2010.

[30] A. Şeker, T. Shahwan, A. E. Eroğlu, S. Yılmaz, Z. Demirel, and M. C. Dalay, "Equilibrium, thermodynamic and kinetic studies for the biosorption of aqueous lead(II), cadmium(II) and nickel(II) ions on *Spirulina platensis*," *Journal of Hazardous Materials*, vol. 154, no. 1–3, pp. 973–980, 2008.

[31] F. Granados-Correa, J. Vilchis-Granados, M. Jiménez-Reyes, and L. A. Quiroz-Granados, "Adsorption behaviour of La(III) and Eu(III) ions from aqueous solutions by hydroxyapatite: kinetic, isotherm, and thermodynamic studies," *Journal of Chemistry*, vol. 2013, Article ID 751696, 9 pages, 2013.

[32] M. S. Chiou and H. Y. Li, "Adsorption behavior of reactive dye in aqueous solution on chemical cross-linked chitosan beads," *Chemosphere*, vol. 50, no. 8, pp. 1095–1105, 2003.

[33] I. Smičiklas, A. Onjia, S. Raičević, Đ. Janaćković, and M. Mitrić, "Factors influencing the removal of divalent cations by hydroxyapatite," *Journal of Hazardous Materials*, vol. 152, no. 2, pp. 876–884, 2008.

[34] F.-C. Wu, R.-L. Tseng, and R.-S. Juang, "Initial behavior of intraparticle diffusion model used in the description of adsorption kinetics," *Chemical Engineering Journal*, vol. 153, no. 1–3, pp. 1–8, 2009.

[35] B. H. Hameed, J. M. Salman, and A. L. Ahmad, "Adsorption isotherm and kinetic modeling of 2,4-D pesticide on activated carbon derived from date stones," *Journal of Hazardous Materials*, vol. 163, no. 1, pp. 121–126, 2009.

[36] M. Greluk and Z. Hubicki, "Sorption of SPADNS azo dye on polystyrene anion exchangers: equilibrium and kinetic studies," *Journal of Hazardous Materials*, vol. 172, no. 1, pp. 289–297, 2009.

[37] O. M. M. Freitas, R. J. E. Martins, C. M. Delerue-Matos, and R. A. R. Boaventura, "Removal of Cd(II), Zn(II) and Pb(II) from aqueous solutions by brown marine macro algae: kinetic modelling," *Journal of Hazardous Materials*, vol. 153, no. 1-2, pp. 493–501, 2008.

[38] A. Selatnia, M. Z. Bakhti, A. Madani, L. Kertous, and Y. Mansouri, "Biosorption of Cd^{2+} from aqueous solution by a

NaOH-treated bacterial dead *Streptomyces rimosus* biomass," *Hydrometallurgy*, vol. 75, no. 1–4, pp. 11–24, 2004.

[39] K. Urano and H. Tachikawa, "Process development for removal and recovery of phosphorus from wastewater by a new adsorbent. II. Adsorption rates and breakthrough curves," *Industrial & Engineering Chemistry Research*, vol. 30, no. 8, pp. 1897–1899, 1991.

[40] M. S. Bilgili, "Adsorption of 4-chlorophenol from aqueous solutions by xad-4 resin: isotherm, kinetic, and thermodynamic analysis," *Journal of Hazardous Materials*, vol. 137, no. 1, pp. 157–164, 2006.

[41] R. Aravindhan, J. R. Rao, and B. U. Nair, "Removal of basic yellow dye from aqueous solution by sorption on green alga *Caulerpa scalpelliformis*," *Journal of Hazardous Materials*, vol. 142, no. 1-2, pp. 68–76, 2007.

[42] Z. Aksu, "Determination of the equilibrium, kinetic and thermodynamic parameters of the batch biosorption of nickel(II) ions onto *Chlorella vulgaris*," *Process Biochemistry*, vol. 38, no. 1, pp. 89–99, 2002.

[43] A. Babarinde, J. O. Babalola, J. Adegoke et al., "Biosorption of Ni(II), Cr(III), and Co(II) from solutions using *Acalypha hispida* leaf: kinetics, equilibrium, and thermodynamics," *Journal of Chemistry*, vol. 2013, Article ID 460635, 8 pages, 2013.

[44] S. Lazarević, I. Janković-Častvan, V. Djokić, Z. Radovanović, D. Janaćković, and R. Petrović, "Iron-modified sepiolite for Ni^{2+} sorption from aqueous solution: an equilibrium, kinetic, and thermodynamic study," *Journal of Chemical & Engineering Data*, vol. 55, no. 12, pp. 5681–5689, 2010.

[45] V. K. Gupta, R. Jain, T. A. Saleh, A. Nayak, S. Malathi, and S. Agarwal, "Equilibrium and thermodynamic studies on the removal and recovery of Safranine-T dye from industrial effluents," *Separation Science and Technology*, vol. 46, no. 5, pp. 839–846, 2011.

[46] W. Guan, J. Pan, H. Ou et al., "Removal of strontium(II) ions by potassium tetratitanate whisker and sodium trititanate whisker from aqueous solution: equilibrium, kinetics and thermodynamics," *Chemical Engineering Journal*, vol. 167, no. 1, pp. 215–222, 2011.

[47] M. Bhaumik, T. Y. Leswifi, A. Maity, V. V. Srinivasu, and M. S. Onyango, "Removal of fluoride from aqueous solution by polypyrrole/F_3O_4 magnetic nanocomposite," *Journal of Hazardous Materials*, vol. 186, no. 1, pp. 150–159, 2011.

[48] M. Chiban, A. Soudani, F. Sinan, and M. Persin, "Single, binary and multi-component adsorption of some anions and heavy metals on environmentally friendly *Carpobrotus edulis* plant," *Colloids and Surfaces B: Biointerfaces*, vol. 82, no. 2, pp. 267–276, 2011.

[49] I. Langmuir, "The adsorption of gases on plane surfaces of glass, mica and platinum," *Journal of the American Chemical Society*, vol. 40, no. 9, pp. 1361–1403, 1918.

[50] Ü. Geçgel, G. Özcan, and G. Ç. Gürpınar, "Removal of methylene blue from aqueous solution by activated carbon prepared from pea shells (*Pisum sativum*)," *Journal of Chemistry*, vol. 2013, Article ID 614083, 9 pages, 2013.

[51] A. Rafique, M. A. Awan, A. Wasti, I. A. Qazi, and M. Arshad, "Removal of fluoride from drinking water using modified immobilized activated alumina," *Journal of Chemistry*, vol. 2013, Article ID 386476, 7 pages, 2013.

[52] S. S. Majumdar, S. K. Das, R. Chakravarty, T. Saha, T. S. Bandyopadhyay, and A. K. Guha, "A study on lead adsorption by *Mucor rouxii* biomass," *Desalination*, vol. 251, no. 1–3, pp. 96–102, 2010.

[53] N. Y. Mezenner, A. Hamadi, S. Kaddour, Z. Bensaadi, and A. Bensmaili, "Biosorption behavior of basic red 46 and violet 3 by dead *Pleurotus mutilus* from single- and multicomponent systems," *Journal of Chemistry*, vol. 2013, Article ID 965041, 12 pages, 2013.

[54] T. Shanthi and V. M. Selvarajan, "Removal of Cr(VI) and Cu(II) ions from aqueous solution by carbon prepared from Henna leaves," *Journal of Chemistry*, vol. 2013, Article ID 304970, 6 pages, 2013.

[55] R. Zein, R. Suhaili, F. Earnestly, I. Indrawati, and E. Munaf, "Removal of Pb(II), Cd(II) and Co(II) from aqueous solution using *Garcinia mangostana* L. fruit shell," *Journal of Hazardous Materials*, vol. 181, no. 1–3, pp. 52–56, 2010.

[56] C. Mahamadi and T. Nharingo, "Utilization of water hyacinth weed (*Eichhornia crassipes*) for the removal of Pb(II), Cd(II) and Zn(II) from aquatic environments: an adsorption isotherm study," *Environmental Technology*, vol. 31, no. 11, pp. 1221–1228, 2010.

[57] J. Anwar, U. Shafique, Waheed-uz-Zaman, M. Salman, A. Dar, and S. Anwar, "Removal of Pb(II) and Cd(II) from water by adsorption on peels of banana," *Bioresource Technology*, vol. 101, no. 6, pp. 1752–1755, 2010.

[58] M. Ghaedi, G. R. Ghezelbash, F. Marahel, S. Ehsanipour, A. Najibi, and M. Soylak, "Equilibrium, thermodynamic, and kinetic studies on lead (II) biosorption from aqueous solution by *Saccharomyces cerevisiae* biomass," *CLEAN—Soil, Air, Water*, vol. 38, no. 9, pp. 877–885, 2010.